Characterization Of Temperature Gradient Driven Turbulence And Transport

M. Ottaviani 1), E. Fleurence 1), X. Garbet 1), Ph. Ghendrih 1), V. Grandgirard 1), B. Labit 1), Y. Sarazin 1), W. Zwingmann 1), P. Bertrand 2), G. Depret 3), A. Ghizzo 2) and G. Manfredi 2)

1) Ass. EURATOM-CEA, DSM/DRFC, 13108 St Paul-lez-Durance , France

2) Laboratoire de Physique des Milieux Ionisés, Université Henri Poincaré, Nancy-1, BP 239 F-54506 Vandoeuvre-les-Nancy cedex, France

3) INRIA Lorraine/Equipe ISA, BP 101, 54602 Vandoeuvre les Nancy, France

e-mail contact of the first author: mao@drfc.cad.cea.fr

Abstract. We report on extensive numerical studies aimed at characterizing various aspects of temperature gradient driven turbulence. We specifically discuss results from 3D fluid models of ETG and of ITG turbulence, and results from a 2D+1D gyro-kinetic model of trapped ion turbulence. Global transport exhibits gyro-Bohm scaling in both the ETG and the ITG model. The conductivity of the ETG model decreases weakly with beta. The heat transport is due to the $\mathbf{E}\times\mathbf{B}$ advection, the effect of the magnetic flutter is found negligible. However the transport level is much lower than experimentally observed. In both 3D models the correlation lengths scale with the gyro-radius, but they are typically a factor 10 larger. Vortices are elongated but their aspect ratio is independent of the gyro-radius. Their radial size is limited by LD. The trapped ion model gives larger vortices due to the absence of LD from passing ions. Avalanches are observed in all the models, the weakest occurring in the ITG system. Their range increases with gyro-radius, but more weakly than linearly. Finally, ZFs can limit the range of the avalanches, which explains why avalanches are weaker in the ITG model which is more sensitive to ZFs.

1. Introduction

This work is dedicated to the extensive numerical work aimed at characterizing the turbulence generated by temperature gradients, the main cause of anomalous heat transport in tokamak plasmas. A common feature of these studies is the use of global direct simulation codes where the profiles evolve self-consistently: boundary conditions are either a prescribed energy flux, or fixed temperature. Since no single code can yet comprehensively simulate the plasma turbulence in the wide spectral range observed in the experiments, the analysis had to be limited to models treating independently the relevant dynamics in various spectral subranges. More specifically, we report here results from the following models: 1) a three dimensional (3D), three-field, electromagnetic fluid model of electron temperature gradient (ETG) driven turbulence, valid for wavelengths below the ion Larmor radius; 2) a 3D, three-field, electrostatic fluid model of ion temperature gradient (ITG) driven turbulence, valid for wavelengths above the ion Larmor radius; 3) a 2+1 dimensional gyro-kinetic model of low-frequency, bounce-averaged, trapped ion turbulence; for this, a semi-Lagrangian code [1] is employed. Below are summarized those findings that are more relevant for the extrapolation to the next step and/or for the understanding of the universal aspects of transport.

2. Global scaling

The effective (electron or ion) thermal conductivity χ is found to exhibit gyro-Bohm scaling for both the ETG [2] and the ITG [3] model, $\chi \sim \rho_*$, where ρ_* is the relevant normalized gyro radius (electron or ion, respectively). Convergence to gyro-Bohm scaling was also reported in recent global gyro-kinetic simulations of ITG turbulence by Lin *et al* [4], finally resolving a longstanding problem. It is important to note that gyro-Bohm scaling becomes apparent only in the limit of sufficiently small ρ_*. Whether ρ_* is small enough depends in general on the choice of the other simulation parameters. A first criterion for the validity of the gyro-Bohm limit is that scale separation must be good; this requires in particular that $\lambda_c \ll L_T$, where λ_c is the turbulence correlation length and L_T the gradient scale length. By employing the estimate $\lambda_c \sim 1/k_r \sim 1/k_\theta$, with $k_\theta \rho_s \approx L_T/qR$, as discussed below, one finds $\rho_* \ll {L_T}^2/(qaR)$, which is a small number, especially for steep gradients (this estimate implicitly assumes that the characteristic poloidal and radial scale-lengths depend on ρ_* in the same way, which is confirmed by the simulations as discussed below.) By evaluating ${L_T}^2/(qaR)$ from the parameters of the simulations given in Ref. [3] and in Ref. [4], one finds that ${L_T}^2/(qaR)$ is about a factor 5 smaller in Ref. [4], which may explain why convergence to gyro-Bohm is achieved at smaller ρ_* in Ref. [4]. Another important difference is that flat density profiles are adopted in Ref. [3]. It is known that corrections to the gyro-Bohm scaling due to finite ρ_* depend on the diamagnetic flow, as discussed by Garbet and Waltz in Ref. [5] and subsequent work. Assuming an expansion of χ in powers of ρ_*, $\chi = \chi_1 \rho_* - \chi_2 \rho_*^2 + ...$, the coefficient χ_2 turns out proportional to the inverse scale-length of the equilibrium profiles, and it is therefore larger for peaked profiles. Smaller values of ρ_* are then required for convergence.

The scaling with the plasma β has been studied for the ETG model, where it enters naturally through the normalized collisionless electron skin depth $d_* = {\rho_*}_e/\beta^{1/2}$. The resulting conductivity decreases weakly with β. One of the motivations of this study was the fast wave electron heating experiment in Tore Supra [6], where the dependence of the empirical conductivity on density and temperature is optimally given by $\chi \sim T^{1/2}/n$, which is consistent with the Okhawa scaling $\chi \sim \rho_*/\beta$, which can be derived heuristically from the ETG model by assuming that the important scale length is the skin depth. The actual numerically found β dependence is weaker (Fig. 1) and the conductivity substantially smaller and mainly due to the electric field fluctuations; transport due to the magnetic flutter is even smaller. Previous flux-tube gyro-kinetic simulations by Jenko *et al* [7] had reported the existence of a regime of enhanced transport associated with the formation of streamers. To date, we are unable to confirm this finding, although turbulent structures of comparable radial size were observed with the ETG code.

3. Characteristics of the fluctuations

By inspecting the equal time correlation functions one finds that the fluctuations produced in the ITG and the ETG models are microscopic, in the sense that all the important scales, like the correlation lengths, are proportional to the gyro-radius, although somewhat larger. ETG vortices are generally somewhat radially elongated, as clearly seen by computing the normalized 2D self-correlation function in the poloidal plane $C(r, \theta)$ (Fig. 3). Their aspect ratio depends weakly on ρ_*. An estimate of the correlation length is obtained by measuring the major axis of the ellipse corresponding to $C(r, \theta) = 0.5$. This gives typically

$\lambda_c \approx 10\rho_*$. ITG vortices are comparatively smaller and their aspect ratio is close to unity except when the injected flux is so small that the temperature profile is near marginality. The roundedness of ITG structures is consistent with the fact that the ITG vortices are more sensitive to zonal flows (ZFs). In the ETG model there seem to be a tendency to isotropization as the injected flux is increased. It is useful to recall that isotropization was often observed in 2D simulations in the '80s, that employed an ETG-like the density response to potential fluctuations (see Ref. [8]).
The finding that the vortices are proportional to the Larmor radius is in agreement with the condition that Landau damping (LD) from passing particles must be weak, $\omega_* > k_\| v_{th}$, in order that turbulence be excited. In the region of closed magnetic surfaces $k_\|$ must have, on average, a lower bound, due to the topologic constraint of the double periodicity and the presence of magnetic shear. Typically $k_\| \sim 1/qR$. When combined with the Landau condition, this gives a minimum wavenumber $k_\theta \rho_s \approx L_T/qR$. It turns out that, due to the inverse cascade, the observed numerical spectrum peaks at a value consistent with this estimate, which is also in agreement with experiments. One also remarks the difference between the 3D ETG/ITG models and the trapped ion model; the latter gives large-scale vortices due to the absence of LD from passing ions, as it can be seen in Fig. 4 (left).

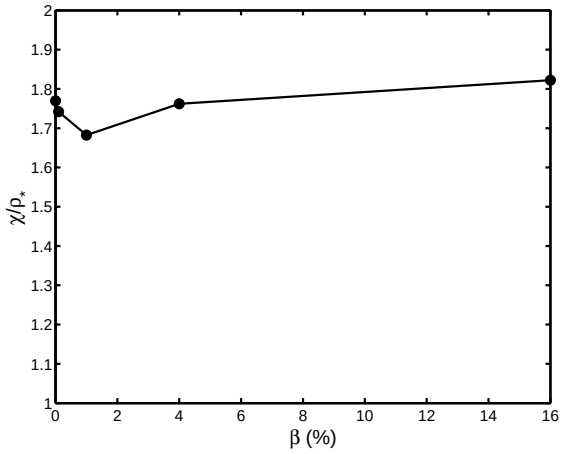

Figure 1: *Dependence of the electron heat conductivity, in gyro-Bohm units, on β (ETG model).*

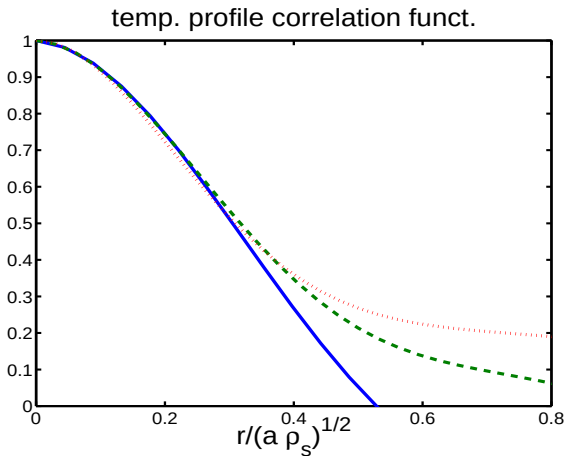

Figure 2: *Correlation functions of the temperature profile obtained from ITG simulations at $\rho_* = 1/50$ (blue solid line), $\rho_* = 1/100$ (green dashed line) and $\rho_* = 1/200$ (red dotted line)*

4. Space-time correlations and intermittency

The phenomenon of avalanches, rapid radial propagation of energy over a large distance, is well documented, to a different degree, in all the above models, the strongest events occurring in the 2D cases and the weakest in the ITG system. The analysis is carried out in the (r, t) plane by computing the space-time correlation of the temperature profile fluctuations. One interesting question is the dependence of the range of the avalanches on the parameter ρ_* for those models that exhibit gyro-Bohm scaling. Fig. 2 shows the radial correlation function of the *temperature profile fluctuations*, obtained from ITG simulations at three values of $\rho_* = 1/50, 1/100$, and $1/200$. In order to superpose the three

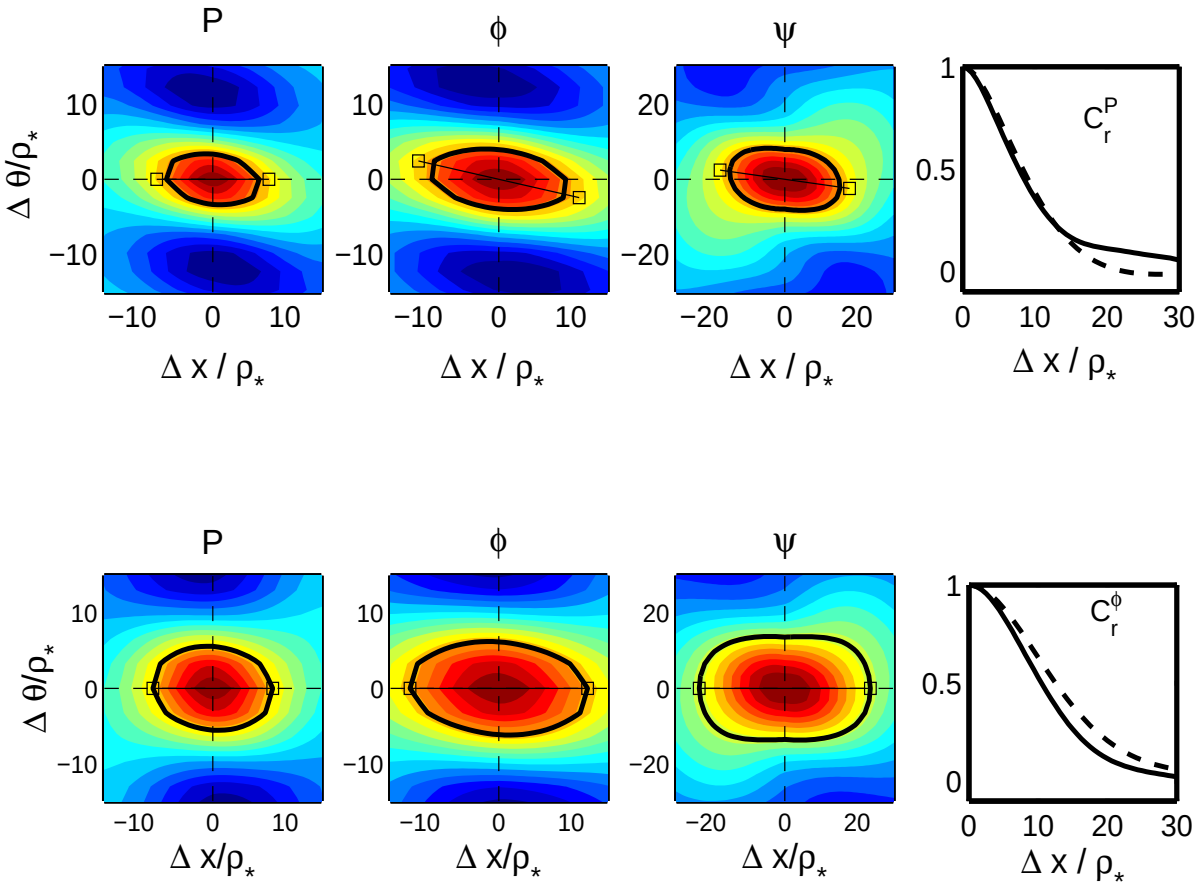

Figure 3: *ETG Two-dimensional correlation functions in the poloidal plane, of (left to right) pressure, electric potential, and magnetic potential, obtained from ETG simulations at* $\rho_* = 1/50$ *(upper row) and* $\rho_* = 1/100$ *(lower row). The comparison of the radial correlation function for the two values of* ρ_* *is shown in the rightmost column. All the lengths are normalized to the Larmor radius.* $\beta = 0.01$ *in all cases.*

curves we had to normalize the abscissa to $\rho_*^{1/2}$. Thus the range of the avalanches seems to scale like $\rho_*^{1/2}$ rather than ρ_*. The reason of this behavior is presently not understood. In any event it suggests that the avalanches observed in the ITG model are not linked to a particular vortex size; they are the consequence of intrinsic space-time correlations, as found in certain sandpile models [9] In general it is important to determine the parametric dependence of the range of the avalanches since it may ultimately determine the scale above which turbulent transport can be treated as a diffusion process. More information on the intermittency was also obtained by studying the probability distribution function of the instantaneous correlation length, which exhibits long tails. Finally, one finds that zonal flows (ZFs), depending on their strength, can limit the range of the avalanches, which may explain why avalanches are weaker in the ITG model where turbulence is more sensitive to ZFs. The 2D trapped ion model exhibits this behavior to the extreme. When the electron response is taken to vanish for zonal modes, i.e. for electric potential fluctuations constant on magnetic surfaces, zonal flows appear to dominate. The system then bifurcates from streamer-like structures which maximize the transport (Fig. 4 left), to zonal modes which completely suppress the transport (Fig. 4 right).

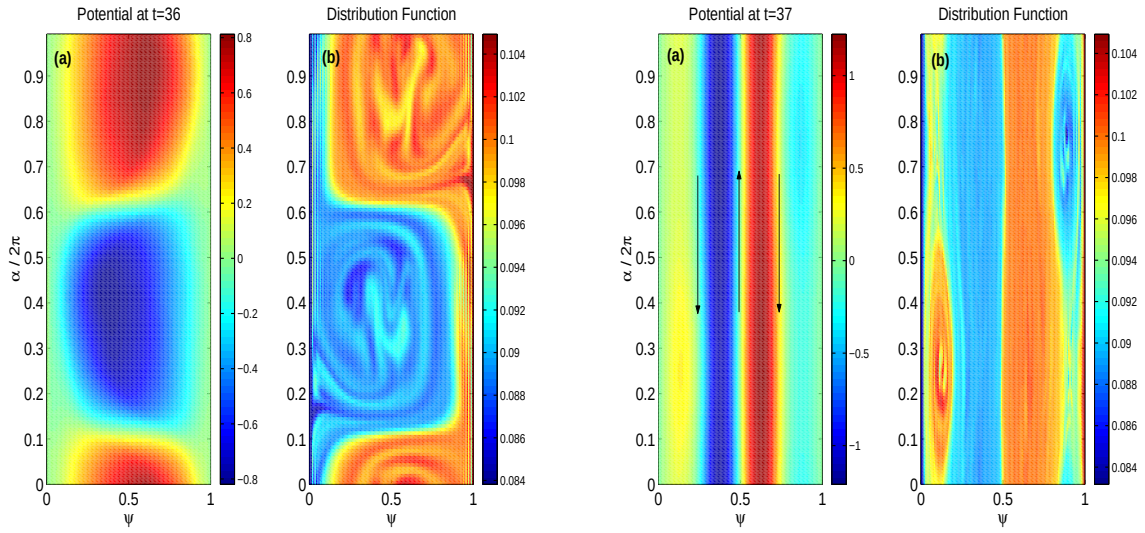

Figure 4: *Potential isolines and distribution function of the 2D gyro-kinetic trapped ion model, (left) without ZFs and (right), with ZFs*

References

[1] DEPRET G., X. GARBET X., BERTRAND P., GHIZZO A., Plasma Phys. Contr. Fusion **42**, 949 (2000).
[2] LABIT B. and OTTAVIANI M., Global numerical study of electron temperature gradient driven turbulence and transport scaling, Phys. of Plasmas (in press)
[3] OTTAVIANI M. and MANFREDI G., Phys. of Plasmas **8**, 3267 (1999).
[4] LIN Z., ETHIER S., HAHM T. S. and TANG W. M., Phys. Rev. Lett. **88**, 195004 (2002).
[5] GARBET X. and WALTZ R. **3**, 1898 (1996).
[6] HOANG G. T., et al., Phys. Rev. Lett. **87**, 125001 (2001).
[7] JENKO F., DORLAND B., KOTSCHENREUTHER M., ROGERS B. N., Phys. of Plasmas **7**, 1904 (2000).
[8] OTTAVIANI M., et al., Phys of Fluids **B2**, 67 (1990)
[9] NEWMAN D. E., CARRERAS B. A., DIAMOND P. H. AND HAHM T. S., Phys. Plasmas **3**, 1858 (1996)